Computationally efficient demographic history inference from allele frequencies with supervised machine learning

Linh N. Tran,[1,2] Connie K. Sun,[2] Travis J. Struck,[2] Mathews Sajan,[2] and Ryan N. Gutenkunst[2,*]

[1]*Genetics Graduate Interdisciplinary Program and* [2]*Department of Molecular & Cellular Biology, University of Arizona, Tucson, AZ, USA.*

***Correspondence:** Ryan N. Gutenkunst, Department of Molecular & Cellular Biology, University of Arizona, Tucson, AZ, 85721, USA. E-mail: rgutenk@arizona.edu.

Abstract

Inferring past demographic history of natural populations from genomic data is of central concern in many studies across research fields. Previously, our group had developed dadi, a widely used demographic history inference method based on the allele frequency spectrum (AFS) and maximum likelihood optimization. However, dadi's maximum likelihood optimization procedure is computationally expensive. Here, we developed donni (demography optimization via neural network inference), a new inference method based on dadi that is more efficient while maintaining comparable inference accuracy. For each dadi-supported demographic model, donni simulates the expected AFS and trains a multilayer perceptron algorithm to infer the model parameters from input AFS. We demonstrated that for many demographic models, donni can infer some parameters, such as population size changes and inbreeding coefficients, very well ($\rho \approx 0.9$) and other parameters, such as migration rates and times of demographic events, fairly well ($\rho \approx 0.6 - 0.7$). Importantly, donni provides parameter inference instantaneously from input AFS, with accuracy comparable to parameters inferred by dadi's likelihood optimization while bypassing its long and computationally intensive evaluation process. Donni's performance demonstrates that supervised machine learning algorithms may be a promising avenue for developing more sustainable and computationally efficient demographic history inference methods.

INTRODUCTION

Inferring demographic history from genomic data has become routine in many research fields, from elucidating the anthropological origins and migration patterns of modern and archaic human populations (Gutenkunst et al. 2009; Bergström et al. 2020; Marchi et al. 2022; Gopalan et al. 2022), to inferring the population genetic trajectories of endangered animals (Mays Jr et al. 2018; Miller-Butterworth et al. 2021; Chavez et al. 2022). Accounting for demographic history is also essential in setting the appropriate background for detecting signals of natural selection (Nielsen et al. 2005; Boyko et al. 2008; Kim et al. 2017), disease associations (Mathieson & McVean 2012), and recombination hotspots (Johnston & Cutler 2012). Due to the wide range of possible demographic models and high dimensionality of genome sequence data, such analysis often involves computationally expensive modeling. As the size of genomic datasets rapidly grows to thousands of full genomes, there is a great need for more efficient and scalable methods for extracting information from such datasets.

One class of widely used methods infers demographic history from sequence data summarized as an allele frequency spectrum (AFS). An AFS is a multidimensional array with dimension equal to the number of populations being considered in a given demographic model. Each array entry is the number of observed single nucleotide polymorphisms (SNP) with given frequencies the sampled populations. For example, the [1,2] entry would count SNPs that were singletons in the first population and doubletons in the second. A major advantage of using the AFS as a summary statistic is the ease of scaling to whole genome data (Marchi et al. 2021), as it efficiently reduces the high dimension of population genomic data. AFS-based inference methods are, therefore, often fast and suitable for exploring many demographic models (Spence et al. 2018). Given its wide use in countless empirical studies, much progress has been made towards understanding the theoretical guarantees and limitations of the AFS and AFS-based inference (Myers et al. 2008; Achaz 2009; Bhaskar & Song 2014; Terhorst & Song 2015; Baharian & Gravel 2018).

Demographic inference methods based on the AFS often work by fitting the observed AFS to its expected value under a user-specified demographic history model with parameters such as population sizes, migration rates, and divergence times. The expected AFS can be computed via a

wide range of approaches (Gutenkunst et al. 2009; Naduvilezhath et al. 2011; Lukić & Hey 2012; Excoffier et al. 2013; Kern & Hey 2017; Jouganous et al. 2017; Kamm et al. 2017) with varying degrees of computational expense, model flexibility, and scalability. Because this is the most computationally intensive step in the procedure, new methods developed thus far have focused on devising algorithms to speed up AFS calculation (Jouganous et al. 2017; Kamm et al. 2017, 2020). However, not much attention has been given to optimizing the way in which the computed AFS is stored and used for inference. In a typical likelihood optimization procedure, hundreds to thousands of expected AFS are computed and compared to the data to obtain the best fit parameter set. These generated AFS and their corresponding demographic parameters contain information regarding the mapping between the AFS and demographic parameters, but are discarded after each optimization run. As there are often a few common demographic models regularly used across studies, if these simulated data could be captured, stored, and distributed for future use, individual groups as well as the research community as a whole could save a lot of time and computational effort by avoiding unnecessary repetition.

The mapping between the AFS and its associated demographic history model parameters can be efficiently captured by supervised machine learning (ML) algorithms. Given a training data set with feature vectors (AFS — input) and labels (demographic history parameters — output), these algorithms can learn the function mapping from the input to the output. While training ML algorithms can be computationally intensive up front, subsequent inference from trained models will have minimal cost (Schrider & Kern 2018). ML algorithms have been widely adopted in population genetics over the past decade, thanks to their efficiency and flexibility. Several studies have used supervised ML algorithms such as random forest (RF) and multilayer perceptron (MLP) with AFS as training data for demographic model selection and demographic parameter inference (Sheehan & Song 2016; Smith et al. 2017; Villanea & Schraiber 2019; Mondal et al. 2019; Lorente-Galdos et al. 2019; Sanchez et al. 2021). In Smith et al. (2017) specifically, the RF algorithm was used to replace the rejection step in the approximate Bayesian computation (ABC) framework, significantly improving overall efficiency (Pudlo et al. 2016). This improvement in efficiency was in part due to more efficient use of simulated data. Whereas in a typical ABC procedure, any

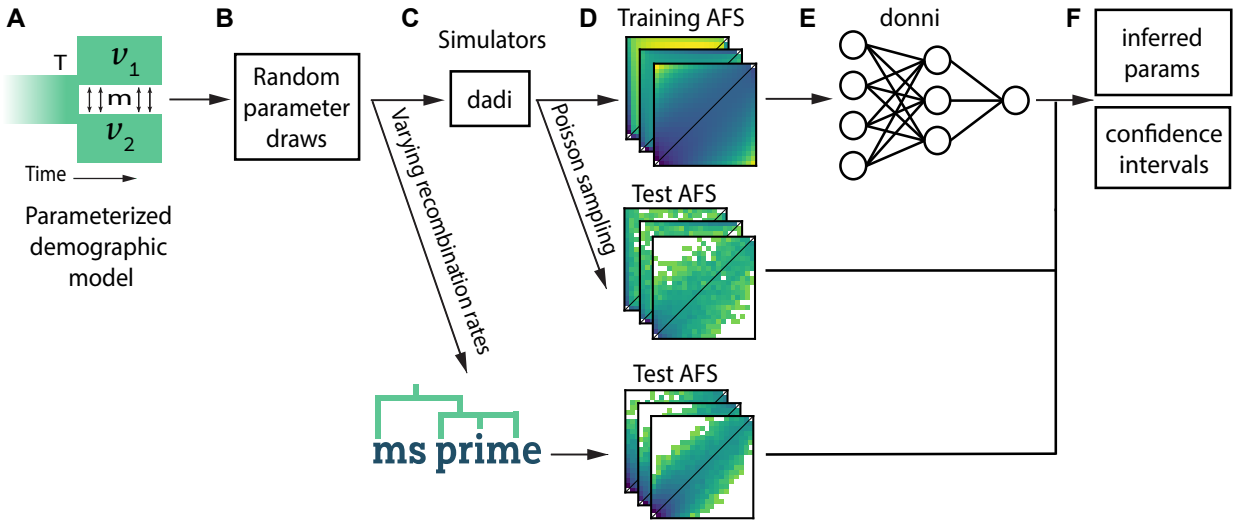

Figure 1: **Schematic of the workflow for training and testing donni.** For a given demographic model (A), we drew sets of model parameters (B) from a biologically relevant range (Table 1). Each parameter set represents a demographic history and corresponds to an expected AFS. These parameters were input into simulator programs (C) to generate training and test AFS (D). We use the expected AFS simulated with dadi and their corresponding parameters as training data for donni (E). We generated test data either by Poisson sampling from dadi-simulated AFS or by varying recombination rates with msprime, resulting in a change in variance compared to training AFS. The output of donni's trained networks includes both inferred parameters and their confidence intervals (F).

simulations beyond a threshold of difference to the data will be discarded, there all simulations were used as input for training the RF classification algorithm. The same principle can be applied in the maximum likelihood optimization and regression framework, where an ML algorithm can be trained by simulated AFS to provide estimates of demographic parameter values, bypassing likelihood optimization.

NEW APPROACHES

Here, we introduce donni (Demography Optimization via Neural Network Inference), a supervised ML extension to dadi, a widely used AFS-based method for inferring models of demographic history (Gutenkunst et al. 2009) and natural selection (Kim et al. 2017). dadi computes the expected AFS by numerically solving a diffusion approximation to the Wright-Fisher model. While the initial implementation of the software could only handle up to three populations, a recent update supports

up to five populations (Gutenkunst 2021). donni uses dadi to generate AFS and demographic parameter labels for training a multilayer perceptron (MLP) algorithm. Trained MLPs can then be used to instantaneously infer the parameter values of future AFS input data, obviating the need for likelihood optimization (Fig. 1). donni supports a wide range of common demographic parameters that dadi supports, including population sizes, divergence times, continuous migration rates, inbreeding coefficients, and ancestral state misidentification ratios. We show that donni has inference accuracy comparable to dadi but requires less computational resources, even after accounting for the cost of training the MLP algorithms. Our trained MLPs library currently includes all demographic models in the dadi API as well as the models from Portik et al. (2017) pipeline. The supported sample sizes are 10, 20, 40, 80, and 160 chromosomes per population (up to 20 chromosomes only for three-population models). For users who only need to use the trained MLPs for available demographic models, almost no computation is required. For users who require custom models, we also provide our command-line interface pipeline for generating trained models that can save time compared to running likelihood optimization with dadi. Furthermore, the custom models produced can be contributed to our growing library and shared with the community. We also implemented an accompanying method for quantifying uncertainty of the inferred parameter values adapted from conformal prediction methods (Romano et al. 2019; Barber et al. 2021). We show that our uncertainty quantification method has good coverage across demographic models and a biologically realistic range of variance in the AFS.

RESULTS

Variance in allele frequencies affects donni training and performance

Since the AFS is the key input data in our method, we first considered how different levels of variance in the AFS might affect training and performance of the MLPs underlying donni. While the expected AFS computed by dadi under a given set of demographic model parameter gives the mean value of each AFS entry, AFS summarized from observed data will have some variance. We asked whether training the MLP on AFS with some level of variance or AFS with no variance would lead to better overall performance. When generating AFS simulations, we modelled such variance

in the AFS by Poisson-sampling from the expected AFS (examples in Fig. S1A and S2B-D.) We implemented four levels of AFS variance: none, low, moderate, and high in AFS used for training and testing. We then surveyed the inference accuracy for all pairwise combinations for each type of variance in training sets versus test sets.

Overall, we found that MLPs trained on AFS with no to moderate level of variance perform similarly across all variance levels in test AFS (Fig. S3-S6 for the split-migration model). High variance in training AFS led to substantially poorer performance in parameters that are more difficult to infer, such as time and migration rate. The population size change and ancestral state misidentification parameters were the least affected by AFS variance, and inference accuracy remained similarly high across all variance scenarios. We concluded that for subsequent analyses and model library production for donni, we would train using AFS with no variance, since there was no clear benefit from adding an extra variance simulation step in training. For test AFS, we would use AFS with moderate level of variance to better match real data.

donni is efficient and has comparable inference accuracy to dadi

Since we built donni to be an alternative to dadi's likelihood optimization, we compared with dadi in our performance analysis. We validated the inference accuracy of donni for three models: a two-population model with an ancestral population split and symmetric migration between the populations (split-migration model, Fig. 2A), a one-population model with one size change event (two epoch model, Fig. 3A), and a three-population model for human migration out of Africa (the OOA model, Fig. 5A) from Gutenkunst et al. (2009). We also compared the computational efficiency of donni and dadi for two different sample sizes of the split-migration model.

For the split-migration model, donni was able to infer all demographic history parameters with accuracy comparable to dadi (Fig. 2B-I). The population size change parameters ν_1 and ν_2 were inferred very well by both donni (Fig. 2F, G) and dadi (Fig. 2B, C). The time parameter T (Fig. 2D, H) and migration rate m (Fig. 2E, I) were more difficult to accurately infer for both methods, with dadi having trouble optimizing parameter values close to the specified parameter boundary (Fig. 2E). We used Spearman's correlation coefficient ρ to quantify the monotonic relationship between the true

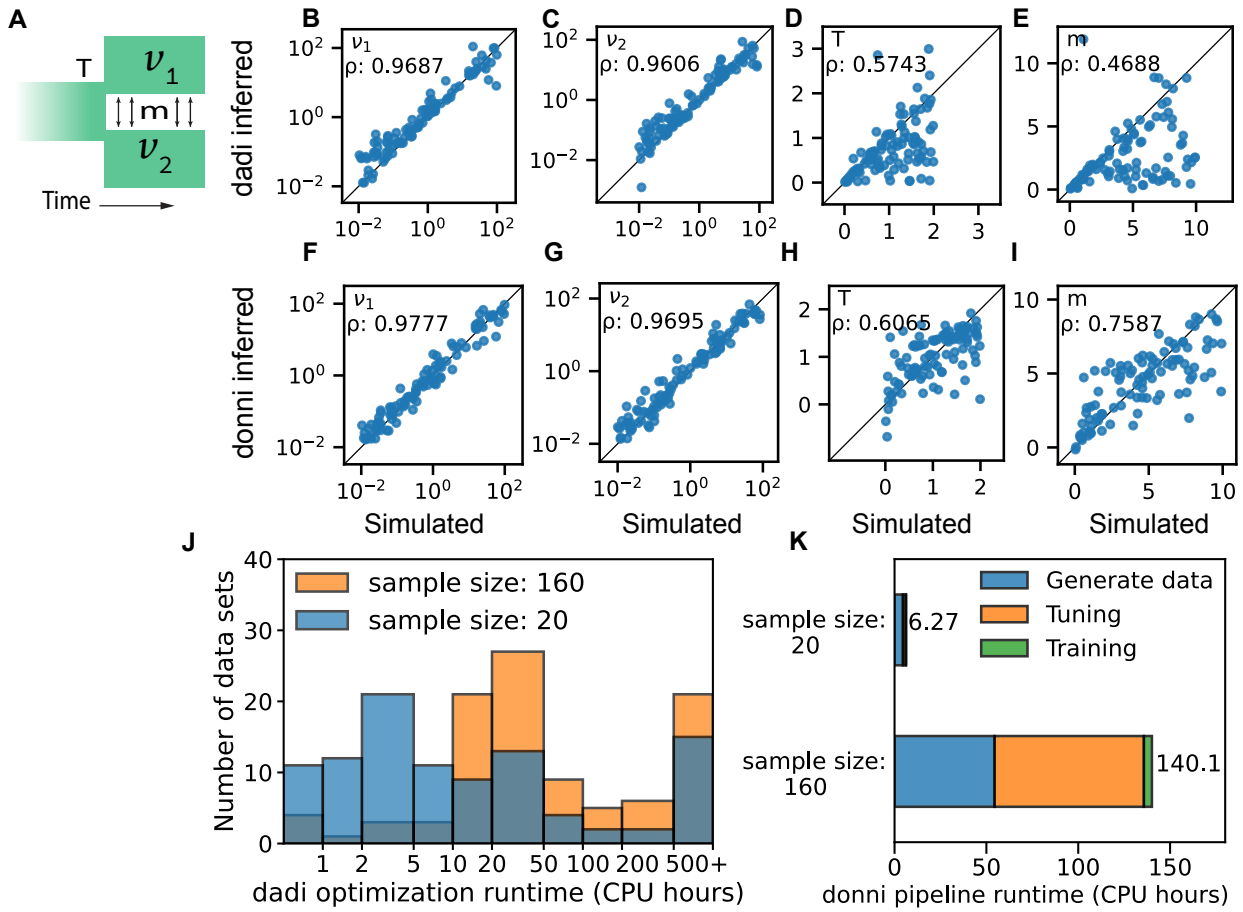

Figure 2: **Inference accuracy and computing time of donni and dadi for a two-population model.** (A) The two-population split-migration model with four parameters: ν_1 and ν_2 are relative sizes of each population to the ancestral, T is time of split, and m is the migration rate. (B-I) Inference accuracy by dadi (B-D) and donni (F-I) for the four parameters on 100 test AFS (sample size of 20). (J) Distribution of optimization times among test data sets for dadi. (K) Computing time required for generating donni's trained MLPs for two sample sizes.

and the inferred parameter values, similar to Flagel et al. (2019). For a more direct measurement of inference accuracy we also provide the RMSE scores for all models in Table S1.

To compare the efficiency of donni and dadi, we benchmarked the computational resources required by each method to infer demographic parameters from the same 100 test AFS (Fig. 2J-K). Since inferring parameters with donni's trained MLPs is computationally trivial, we instead measured the resources required by donni to generate trained MLPs. For both methods, computation was substantially more expensive as the sample size increased from 20 chromosomes to 160. For dadi (Fig. 2J), there was a spread of optimization runtime among the 100 test AFS, with several

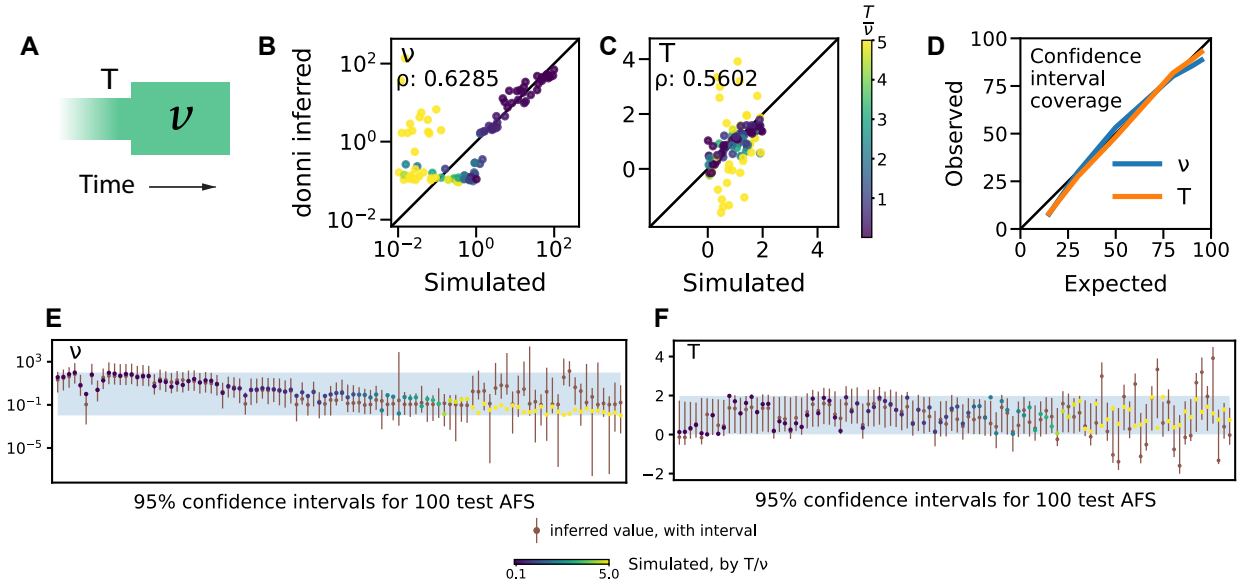

Figure 3: **Uninformative AFS affecting inference accuracy and uncertainty quantification method validation.** (A) The one-population two-epoch model with two parameters, ν for size change and T for time of size change. (B-C) Inference accuracy for ν and T by donni on 100 test AFS, colored by true $\frac{T}{\nu}$ values. (D) Confidence interval coverage for ν and T by donni. The observed coverage is the percentage of test AFS that have true parameter values captured within the corresponding expected interval. (E&F) As an example, we show details of the 95% confidence interval data points from panel D for 100 test AFS. The true values for ν (E) and T (F) of these AFS are colored by $\frac{T}{\nu}$ values, similar to panels B-C. donni's inferred parameter values and 95% confidence interval outputs are in brown. The percentage of true color dots lying within donni's inferred brown interval gives the observed coverage at 95%. The light shades are the true parameter range used in simulating training and test AFS.

difficult spectra requiring more than 500 CPU hours to reach convergence for both sample sizes. By comparison, the computation required for donni (Fig. 2K), including generating training data with dadi and hyperparameter tuning with Hyperband, was less than the average time required for running dadi optimization on a single AFS. This result suggests that donni may benefit many cases where dadi optimization can take a long time to reach convergence.

donni accurately estimates uncertainty of inferred parameter values

Sometimes, demographic model parameters may be unidentifiable, because multiple parameter sets generate nearly identical AFS. As a simple example, we considered the one-population two epoch model (Fig. 3A), which is parameterized by the relative size ν of the contemporary population and the time at which the population size changed T. For this model, donni inferences are inaccurate

when T/ν is large (Fig. 3B-C). In this parameter regime, over the time T after the size change, the AFS relaxes back to that of an constant-sized equilibrium population. Therefore, in this case, the true parameters are unrecoverable because the AFS itself does not have the appropriate signal to infer them. While this problem may be avoided if users follow the best practice for model selection of exploring simpler models before complex ones (Marchi et al. 2021), it also highlights the need for uncertainty quantification, where a wide confidence interval would appropriately indicate problematic inference.

To address this problem, we implemented an accompanying uncertainty quantification method for donni that outputs a confidence interval for each inferred parameter in addition to the point estimate. Our uncertainty method is based on the jackknife+ approach (Barber et al. 2021) implemented by the software package MAPIE (Model Agnostic Prediction Interval Estimator). For the two-epoch model, this approach provided well-calibrated confidence intervals (3D). Considering individual test AFS, the uninformative AFS yielded appropriately wide confidence intervals (Fig. 3E-F, yellow points). We found that confidence intervals were similarly well-calibrated for the split-migration model (Fig. S7).

donni is not biased by linkage between alleles

The Poisson Random Field model underlying dadi (Sawyer & Hartl 1992) and thus donni assumes independence of all genomic loci in the data, which is equivalent to assuming infinite recombination between any pair of loci. But loci within close proximity on the same chromosome are likely sorted together during recombination and therefore linked. To assess how linkage affects donni inference, we tested donni's trained MLPs on AFS simulated with msprime, a coalescent simulator that includes linkage (Baumdicker et al. 2022). These msprime-simulated AFS (examples in Fig. S1B and S2E-G) represent demographic scenarios similar to those in dadi but also include varying levels of linkage under a range of biologically realistic recombination rates. Since smaller recombination rates lead to more linkage and further departure from the training data assumption, we tested donni on AFS with decreasingly small recombination rates down to $r = 10^{-10}$ crossover per base pair per generation, which is two orders of magnitude smaller than the average recombination rate in humans.

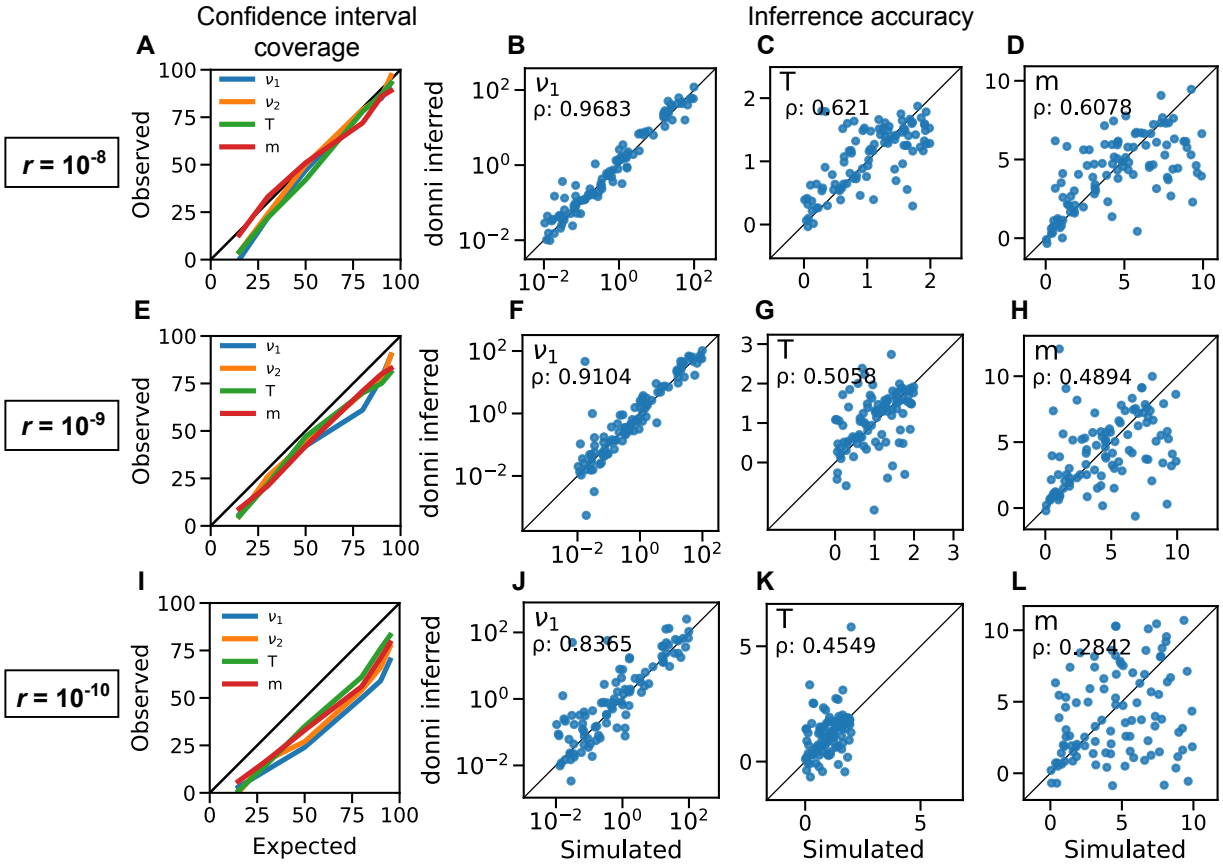

Figure 4: **donni's inference accuracy and uncertainty quantification coverage on msprime-simulated test AFS with linkage.** Each row shows the confidence interval coverage and inference accuracy for select parameters of the split-migration demographic model (Fig. 2A) at varying recombination rate. Recombination rate decreases from top to bottom row, corresponding to increased linkage and variance in the msprime-simulated test AFS.

Population size parameters ν were inferred well no matter the recombination rate, but the inference accuracy for T and m decreased as the recombination rate decreased (Fig. 4). Confidence intervals were well calibrated at the higher recombination rates (Fig. 4A&E), but too small at the lowest recombination rate (Fig. 4I). These patterns are similar to those we found when testing the effects of AFS variance by Poisson-sampling from expected AFS with dadi (Fig.S3-S7), where accuracy decreased with higher variance, and confidence intervals were underestimated at the highest variances. Importantly, even though more linkage did lead to higher variance in the estimated parameter values, we did not observe bias in our inferences.

Comparison with dadi for the Out-of-Africa model

Finally, we tested donni on the three-population Out-of-Africa (OOA) model with 6 size change parameters, 4 migration rates, and 3 time parameters (Fig. 5A). In general, we observed a similar pattern to previous models; size change parameters were often easier to infer than times or migration rates (Fig. 5). For example, both donni and dadi showed near perfect inference accuracy for ν_{Af} (Fig. 5B&G). They both also performed well for the for ν_{Eu}, ν_{As} and *misid* parameters (Fig. S8). But several parameters were challenging for both methods, including some size change parameters, such as ν_{As0} (Fig. 5C,H), ν_B and ν_{Eu0} (Fig. S8). The time parameters proved to be the most challenging with relatively lower accuracy for both methods, with T_{Af} (Fig. 5D,I and T_B S8) being particularly difficult. Overall, both methods agree on the parameters that are easy versus difficult to infer.

However, when inference accuracy is poor on difficult parameters, dadi and donni tend to have different failure patterns. For instance with the m_{AfB} parameter, dadi tended to get stuck at the parameter boundaries for many AFS (Fig. 5E), while donni essentially inferred the average value for all test AFS (Fig. 5J). This indicates a failure by donni to learn any information from the training AFS for this particular parameter. For all other migration rate parameters in the model, donni performs well, matching dadi (Fig. S8).

While performance varied between the two methods among parameters, donni still had comparable accuracy to dadi in most cases. donni was also able to produce well calibrated confidence intervals for all parameters (Fig. 5F). Due to the computational expense of dadi optimization for this

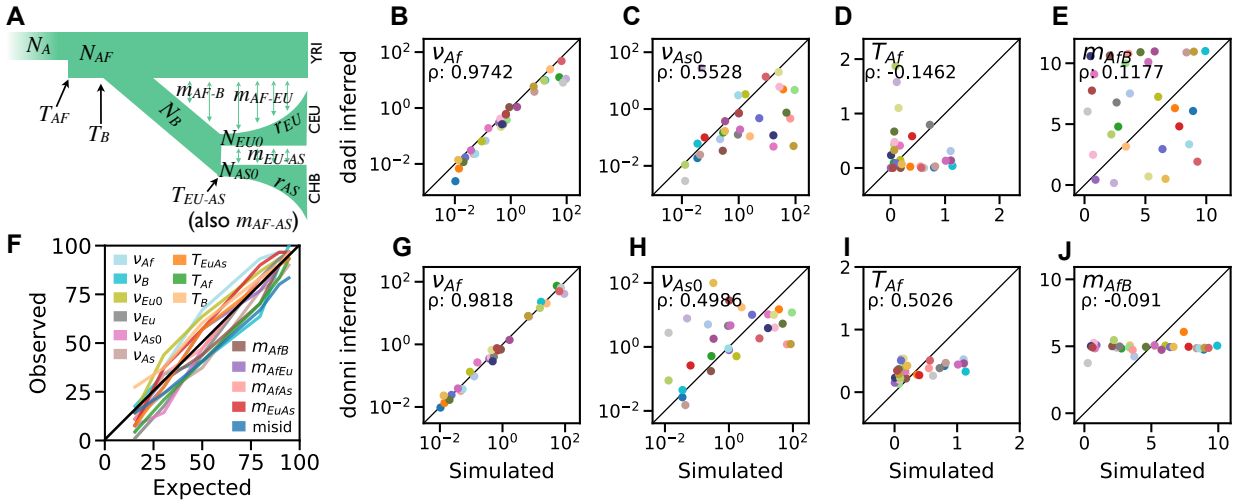

Figure 5: **Inference accuracy compared with dadi and confidence interval coverage by donni for the Out-of-Africa demographic model.** (A) The three-population Out-of-Africa model with 14 demographic history parameters. (B-E) Inference accuracy for representative parameters from 30 test AFS inferred by dadi. (G-J) Inference accuracy for the same parameters and 30 test AFS inferred by donni. For the accuracy of the rest of the parameters see Fig. S8. (F) donni confidence interval coverage for all model parameters.

model, we only analyzed 30 test AFS for direct comparison between donni and dadi. Since donni is not as computationally constrained, we also tested donni on all 1000 test AFS per our standard procedure, finding similar results (S1).

donni's trained MLPs are accessible

Given its speed, we expect that donni will be useful for quickly exploring many demographic scenarios given a user's data set. To support this, we have produced trained MLPs for a large collection demographic history models. These include five one-population and eight two-population models from the current dadi API, plus the 34 two-population and 33 three-population models from Portik et al. (2017). For each of these models, we provide trained MLPs for unfolded and folded AFS for each of five sample sizes (only two sample sizes for three-population models). For large-scale production, we developed a comprehensive command-line interface pipeline for generating training data, tuning hyperparameters, and assessing the quality of the trained MLPs. For hyperparameter tuning, we chose the Hyperband algorithm (Li et al. 2017), which maximizes hyperparameter search with limited resources. donni's pipeline is open-source and available on

GitHub (https://github.com/lntran26/donni) for users interested in training custom models. The trained MLP library is available on CyVerse (Merchant et al. 2016; Center 2011) and donni's command-line interface will automatically download appropriate MLPs.

DISCUSSION

We addressed dadi's computationally intensive optimization procedure by developing donni, a new inference method based on a supervised machine learning algorithm, the multilayer perceptron (MLP). We found that donni can instantaneously infer many demographic history parameters with accuracy comparable to dadi. Even when including computing time required for training the MLP networks, for many cases donni is faster than dadi's maximum likelihood optimization. We also incorporated an accompanying method for uncertainty quantification based on the jacknife+ method (Barber et al. 2021). Through examples of one-, two-, and three-population demographic models, we demonstrated that donni's uncertainty quantification method works well for a wide range of demographic parameters. We also showed that donni works well for AFS simulated by msprime, which includes linkage.

Our approach of using supervised machine learning to reduce computational expense of the maximum likelihood optimization step is similar in spirit to Smith et al. (2017) using random forests to improve the efficiency of the computationally intensive ABC procedure. While Smith et al. (2017) developed a classification approach for demographic model selection, our method is a regression approach, where we provide a suit of pre-trained regressors for many commonly used demographic history models. Users can quickly explore many possible scenarios and get an estimate for several demographic parameters based on their input AFS data. However, we caution users to always start with simpler models first before trying more complex ones, to avoid exacerbating the uninformative parameter space problem. While we have implemented an accompanying uncertainty quantification tool to aid in identifying such problematic scenarios, best practices in model-based inference should still be followed.

Our choice of AFS as input data for training the MLP algorithm has several limitations. First, because the size of the AFS depends on the sample size but the MLP requires a fixed input size,

we have to train a different set of MLPs for different sample sizes within the same demographic history model. Different sets of trained MLPs are also required for unfolded versus folded AFS. We have limited our trained MLP library to sample sizes of 10, 20, 40, 80, and 160 chromosome per population. Users with data that don't match exactly these sample sizes will need to down-project their data AFS, leading to some data loss. It is, however, possible to use donni's pipeline to train custom models that can support a different sample size. We also verified that donni still provides accurate inference and well-calibrated confidence intervals on down-projected data (Fig. S9).

Second, for optimal MLP performance, we need to normalize the AFS data for training, leading to loss of information about the parameter $\theta = 4N_a\mu L$, where N_a is the ancestral effective population size, μ is the mutation rate and L is the sequence length. Estimating θ is required for converting all demographic parameters in genetic units to absolute population sizes and divergence times. While donni can provide a point estimate for θ, it cannot provide the uncertainty, which is necessary for estimating the uncertainty of absolute parameter values. This limitation can be overcome with a hybrid approach between donni and dadi, where donni's inferred parameter outputs become the starting point for dadi's optimization procedure and uncertainty estimation (Coffman et al. 2016). While this approach requires running likelihood optimization, a good starting value provided by donni will reduce overall computing time.

In conclusion, our results indicate that using supervised machine learning algorithms trained with AFS data is a computationally efficient approach for inferring demographic history from genomic data. Despite implementation limitations discussed above, the AFS is fast to simulate compared to other types of simulated data such as genomic sequence images (Flagel et al. 2019; Sanchez et al. 2021) or coalescent trees (Baumdicker et al. 2022; Kelleher et al. 2016). Furthermore, while ignoring linkage may be a weakness of AFS-based methods, it can also be a strength in that it is more species-agnostic and therefore trained models are transferable among species. A major challenge for AFS-based methods such as ours is the poor scaling to large sample sizes and number of populations, where the AFS matrix becomes high dimensional and sparse, and simulation becomes prohibitively expensive. While we limited this study to three-population models, there have been major improvements in AFS-based methods that can handle more (Gutenkunst 2021;

Jouganous et al. 2017; Kamm et al. 2017, 2020). Given our results, a supervised machine learning approach might be a promising next step to extend to such AFS-based methods to further improve their computational efficiency.

MATERIALS AND METHODS

Simulations with dadi

We used dadi v.2.3.0 (Gutenkunst et al. 2009) to simulate AFS for training and testing the MLPs. For each demographic model, we uniformly drew parameter sets from a biologically relevant range of parameters (Table S2). We then generated each expected AFS by specifying the demographic model and parameters in dadi. We calculated the extrapolation grid points used for dadi integration based on the number of chromosomes per population according to Gutenkunst (2021) for one-population models. For models with more than one population, we used the same formula but also increased the grid points by a factor of 1.5 for each additional population. The demographic model parameter values are used as labels for the generated AFS data. To simulate AFS with different levels of variance, we started with the original expected AFS set (no variance). We then Poisson-sampled from the expected AFS to generate a new AFS with variance. We controlled the level of variance by the parameter θ, by which we multiply the expected AFS before sampling. We used $\theta = 10000$, 1000, and 100 corresponding to low, medium, and high levels of variance, respectively (Fig. S3-S7.) Finally, we normalized both expected and Poisson-sampled AFS for training and testing. The results shown in Fig. 2,3,5, and S8 are based on unfolded AFS with sample size of 20 chromosomes per population.

Simulations with msprime

We used msprime v1.2.0 (Baumdicker et al. 2022) to simulate AFS from demographic history models while including linkage. We first specified dadi-equivalent demography in msprime for the two epoch and split-migration models. This included the population size change ratio ν and time of change T parameters for the two epoch model, and population size change ratios ν_1 and ν_2, time T of split, and migration rate m for the split-migration model. We then specified additional parameters required for msprime to yield $\theta = 4N_A L\mu = 40,000$, with ancestral population size $N_A = 10,000$,

sequence length $L = 10^8$ base pairs, and mutation rate $\mu = 10^{-8}$ per base pair per generation. We used three recombination rates 10^{-8}, 10^{-9}, and 10^{-10} per base pair per generation to simulate different levels of linkage and variance in the AFS. We then generated tree-sequence data with msprime before converting to the corresponding unfolded AFS of sample size 20 chromosomes per population and normalizing for testing with trained MLPs.

Network architecture and hyperparameter optimization

We used scikit-learn v1.2.0 `MLPRegressor` to generate all trained networks for donni. These networks are fully-connected feedforward neural networks with one to three hidden layers. Each hidden layer contains between 5 and 50 neurons. The exact number of hidden layers and neurons in each trained network are hyperparameters that were automatically selected via our tuning procedure. The architecture options for tuning depended on the dimension of the input AFS (Table S3), which were flattened before training and testing. All other tuned hyperparameters are listed in Table S4. The default options were used for the rest of the `MLPRegressor` hyperparameters.

For automatic hyperparameter tuning, we implemented the Hyperband algorithm(Li et al. 2017) using the scikit-learn `HalvingRandomSearchCV`. Each band of the HyperBand is a halving random search with a different resource allocation strategy for the same amount of resources. The amount of resources allocated to each band here is controlled by the MLP hyperparameter `max_iter`, which limits the number of maximum iterations allowed per candidate hyperparameter set. This is set to 300 iterations in our pipeline. With the same maximum iterations, the `HalvingRandomSearchCV` in the first band starts with more candidate hyperparameters that run for fewer iterations, while the last band starts with fewer candidates that run for more iterations before elimination based on cross-validation score ranking. The candidate hyperparameter set with the highest cross-validation score across all bands is selected for subsequent MLP training.

Uncertainty quantification coverage

For uncertainty quantification, we used MAPIE v0.6.1 (Quantmetry 2023), a scikit-learn compatible package for confidence interval estimation. With MAPIE, the desired intervals can be specified by the variable `alpha` where `alpha=0.05` corresponds to the 95% confidence interval. To validate our

uncertainty quantification method, we first obtained the method's estimation for six confidence intervals, 15, 30, 50, 80, 90, and 95% on all test AFS. We then get the observed coverage by calculating the percentage of test AFS that have their corresponding simulated parameter value captured within the estimated interval. The expected versus observed percentages are plotted in our confidence interval coverage plots.

donni training and testing pipeline

We used 5,000 AFS for training (no variance) and 1,000 AFS for accuracy and uncertainty coverage validation (moderate variance, $\theta = 1000$). For visualization, only 100 test AFS (30 AFS for the out-of-Africa model) are shown to compare with dadi. However, accuracy scores by donni on all 1000 test AFS are provided in Table S1. Our pipeline tunes and trains one MLP for each demographic model parameter and sample size. For example, the two epoch model with two parameters ν and T has 20 independently trained MLPs: 2 MLPs for ν and T times 5 supported sample sizes times 2 polarization states. Because training can sometimes fail due to the stochasticity of the training optimization algorithm, we implemented an automatic retraining procedure for each demographic model parameter where training is repeated if $\rho \leq 0.2$ on the test data for a maximum of ten retrains.

Likelihood optimization with dadi-cli

To infer demographic parameters for a large number of test AFS in parallel (100 AFS for the split-migration model and 30 AFS for the out-of-Africa model), we used dadi's command-line interface (Huang 2023). We specified the upper and lower bound values for optimization based on the parameter range provided in Table S2. Optimization ran until convergence, as defined by $\delta log(L) = 0.0005$ for the Out-of-Africa model and $\delta log(L) = 0.001$ for the split-migration model.

Benchmarking dadi optimization and donni pipeline

To benchmark the computational expense required for dadi optimization versus for training the MLPs, we used 10 CPUs on a single computing node for each task. For donni, the tasks are generating training AFS, hyperparameter tuning with HyperBand, and training using the tuned hyperparameters. Estimating demographic parameters for 100 test AFS with donni's trained MLPs is nearly instantaneous. For dadi, each test AFS is a task that was optimized until convergence, at

which time was recorded, or until the specified cut-off time (50 hours $\times$ 10 CPUs $=$ 500 CPU hours).

* References

Achaz G (2009) Frequency spectrum neutrality tests: one for all and all for one. Genetics 183:249.

Baharian S, Gravel S (2018) On the decidability of population size histories from finite allele frequency spectra. Theoretical Population Biology 120:42.

Barber RF, Candes EJ, Ramdas A, Tibshirani RJ (2021) Predictive inference with the jackknife+. The Annals of Statistics 49:486.

Baumdicker F, Bisschop G, Goldstein D, Gower G, Ragsdale AP, Tsambos G, Zhu S, Eldon B, Ellerman EC, Galloway JG, et al. (2022) Efficient ancestry and mutation simulation with msprime 1.0. Genetics 220:iyab229.

Bergström A, McCarthy SA, Hui R, Almarri MA, Ayub Q, Danecek P, Chen Y, Felkel S, Hallast P, Kamm J, et al. (2020) Insights into human genetic variation and population history from 929 diverse genomes. Science 367:eaay5012.

Bhaskar A, Song YS (2014) Descartes'rule of signs and the identifiability of population demographic models from genomic variation data. Annals of statistics 42:2469.

Boyko AR, Williamson SH, Indap AR, Degenhardt JD, Hernandez RD, Lohmueller KE, Adams MD, Schmidt S, Sninsky JJ, Sunyaev SR, et al. (2008) Assessing the evolutionary impact of amino acid mutations in the human genome. PLoS genetics 4:e1000083.

Center D (2011) The iplant collaborative: cyberinfrastructure for plant biology. Chardon, M, and Vandewalle, P(1991) Acoustico-lateralis system Cyprinid Fishes .

Chavez DE, Gronau I, Hains T, Dikow RB, Frandsen PB, Figueiró HV, Garcez FS, Tchaicka L, de Paula RC, Rodrigues FH, et al. (2022) Comparative genomics uncovers the evolutionary history, demography, and molecular adaptations of south american canids. Proceedings of the National Academy of Sciences 119:e2205986119.

Coffman AJ, Hsieh PH, Gravel S, Gutenkunst RN (2016) Computationally efficient composite likelihood statistics for demographic inference. Molecular biology and evolution 33:591.

Excoffier L, Dupanloup I, Huerta-Sánchez E, Sousa VC, Foll M (2013) Robust demographic inference from genomic and snp data. PLoS genetics 9:e1003905.

Flagel L, Brandvain Y, Schrider DR (2019) The unreasonable effectiveness of convolutional neural networks in population genetic inference. Molecular biology and evolution 36:220.

Gopalan S, Berl RE, Myrick JW, Garfield ZH, Reynolds AW, Bafens BK, Belbin G, Mastoras M, Williams C, Daya M, et al. (2022) Hunter-gatherer genomes reveal diverse demographic trajectories during the rise of farming in eastern africa. Current Biology 32:1852.

Gutenkunst RN (2021) Dadi. cuda: accelerating population genetics inference with graphics processing units. Molecular biology and evolution 38:2177.

Gutenkunst RN, Hernandez RD, Williamson SH, Bustamante CD (2009) Inferring the joint demographic history of multiple populations from multidimensional snp frequency data. PLoS genetics 5:e1000695.

Huang X (2023) dadi-cli. https://github.com/xin-huang/dadi-cli.

Johnston HR, Cutler DJ (2012) Population demographic history can cause the appearance of recombination hotspots. The American Journal of Human Genetics 90:774.

Jouganous J, Long W, Ragsdale AP, Gravel S (2017) Inferring the joint demographic history of multiple populations: beyond the diffusion approximation. Genetics 206:1549.

Kamm J, Terhorst J, Durbin R, Song YS (2020) Efficiently inferring the demographic history of many populations with allele count data. Journal of the American Statistical Association 115:1472.

Kamm JA, Terhorst J, Song YS (2017) Efficient computation of the joint sample frequency spectra for multiple populations. Journal of Computational and Graphical Statistics 26:182.

Kelleher J, Etheridge AM, McVean G (2016) Efficient coalescent simulation and genealogical analysis for large sample sizes. PLoS computational biology 12:e1004842.

Kern AD, Hey J (2017) Exact calculation of the joint allele frequency spectrum for isolation with migration models. Genetics 207:241.

Kim BY, Huber CD, Lohmueller KE (2017) Inference of the distribution of selection coefficients for new nonsynonymous mutations using large samples. Genetics 206:345.

Li L, Jamieson K, DeSalvo G, Rostamizadeh A, Talwalkar A (2017) Hyperband: A novel bandit-based approach to hyperparameter optimization. The Journal of Machine Learning Research 18:6765.

Lorente-Galdos B, Lao O, Serra-Vidal G, Santpere G, Kuderna LF, Arauna LR, Fadhlaoui-Zid K, Pimenoff VN, Soodyall H, Zalloua P, et al. (2019) Whole-genome sequence analysis of a pan african set of samples reveals archaic gene flow from an extinct basal population of modern humans into sub-saharan populations. Genome biology 20:1.

Lukić S, Hey J (2012) Demographic inference using spectral methods on snp data, with an analysis of the human out-of-africa expansion. Genetics 192:619.

Marchi N, Schlichta F, Excoffier L (2021) Demographic inference. Current Biology 31:R276.

Marchi N, Winkelbach L, Schulz I, Brami M, Hofmanová Z, Blöcher J, Reyna-Blanco CS, Diekmann Y, Thiéry A, Kapopoulou A, et al. (2022) The genomic origins of the world's first farmers. Cell .

Mathieson I, McVean G (2012) Differential confounding of rare and common variants in spatially structured populations. Nature genetics 44:243.

Mays Jr HL, Hung CM, Shaner PJ, Denvir J, Justice M, Yang SF, Roth TL, Oehler DA, Fan J, Rekulapally S, et al. (2018) Genomic analysis of demographic history and ecological niche modeling in the endangered sumatran rhinoceros dicerorhinus sumatrensis. Current Biology 28:70.

Merchant N, Lyons E, Goff S, Vaughn M, Ware D, Micklos D, Antin P (2016) The iplant collaborative: cyberinfrastructure for enabling data to discovery for the life sciences. PLoS biology 14:e1002342.

Miller-Butterworth CM, Diefenbach DR, Edson JE, Hansen LA, Jordan JD, Gingery TM, Russell AL (2021) Demographic changes and loss of genetic diversity in two insular populations of bobcats (lynx rufus). Global Ecology and Conservation 26:e01457.

Mondal M, Bertranpetit J, Lao O (2019) Approximate bayesian computation with deep learning supports a third archaic introgression in asia and oceania. Nature communications 10:1.

Myers S, Fefferman C, Patterson N (2008) Can one learn history from the allelic spectrum? Theoretical population biology 73:342.

Naduvilezhath L, Rose LE, Metzler D (2011) Jaatha: a fast composite-likelihood approach to estimate demographic parameters. Molecular Ecology 20:2709.

Nielsen R, Williamson S, Kim Y, Hubisz MJ, Clark AG, Bustamante C (2005) Genomic scans for selective sweeps using snp data. Genome research 15:1566.

Portik DM, Leaché AD, Rivera D, Barej MF, Burger M, Hirschfeld M, Rödel MO, Blackburn DC, Fujita MK (2017) Evaluating mechanisms of diversification in a guineo-congolian tropical forest frog using demographic model selection. Molecular ecology 26:5245.

Pudlo P, Marin JM, Estoup A, Cornuet JM, Gautier M, Robert CP (2016) Reliable abc model choice via random forests. Bioinformatics 32:859.

Quantmetry (2023) MAPIE - Model Agnostic Prediction Interval Estimator. `https://github.com/scikit-learn-contrib/MAPIE`.

Romano Y, Patterson E, Candes E (2019) Conformalized quantile regression. Advances in neural information processing systems 32.

Sanchez T, Cury J, Charpiat G, Jay F (2021) Deep learning for population size history inference: Design, comparison and combination with approximate bayesian computation. Molecular Ecology Resources 21:2645.

Sawyer SA, Hartl DL (1992) Population genetics of polymorphism and divergence. Genetics 132:1161.

Schrider DR, Kern AD (2018) Supervised machine learning for population genetics: a new paradigm. Trends in Genetics 34:301.

Sheehan S, Song YS (2016) Deep learning for population genetic inference. PLoS computational biology 12:e1004845.

Smith ML, Ruffley M, Espíndola A, Tank DC, Sullivan J, Carstens BC (2017) Demographic model selection using random forests and the site frequency spectrum. Molecular Ecology 26:4562.

Spence JP, Steinrücken M, Terhorst J, Song YS (2018) Inference of population history using coalescent hmms: review and outlook. Current opinion in genetics & development 53:70.

Terhorst J, Song YS (2015) Fundamental limits on the accuracy of demographic inference based on the sample frequency spectrum. Proceedings of the National Academy of Sciences 112:7677.

Villanea FA, Schraiber JG (2019) Multiple episodes of interbreeding between neanderthal and modern humans. Nature ecology & evolution 3:39.

Supporting Information

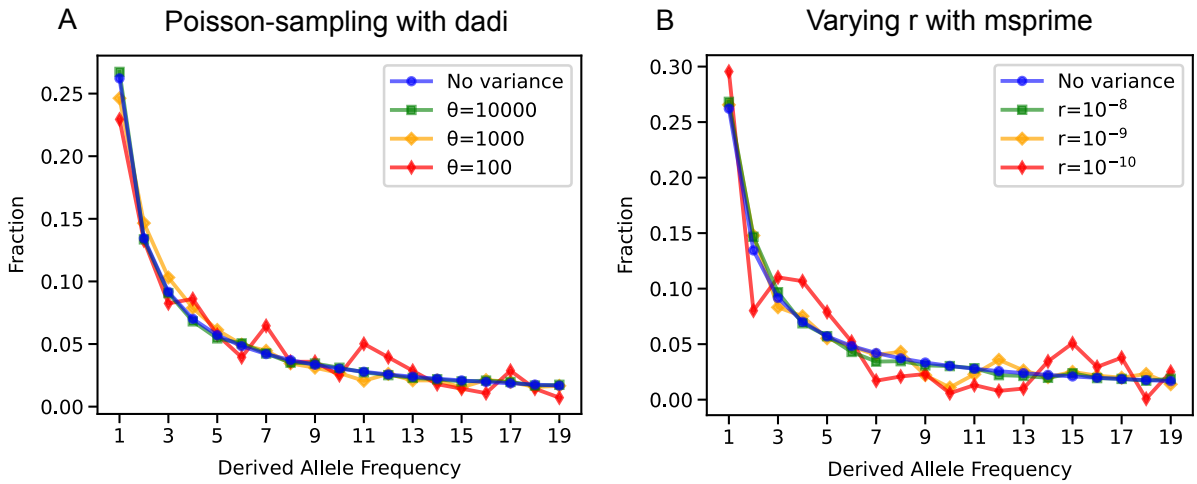

Figure S1: **Simulated AFS examples with different variance for the two epoch model**. All AFS are normalized and plotted on the same scale. The blue "No variance" line with circle dots in both panels is the expected AFS generated by dadi with $\nu = 0.8$, $T = 0.5$ (A) AFS with different variance by Poisson-sampling from the "No variance" AFS. (B) msprime-simulated AFS with equivalent demography to (A) but with varying recombination rates. Here $\theta = 4N_a\mu L = 4 \times 10^3$ (with $\mu = 10^{-8}$ per nucleotide per generation and $L = 10^8$ base pairs).

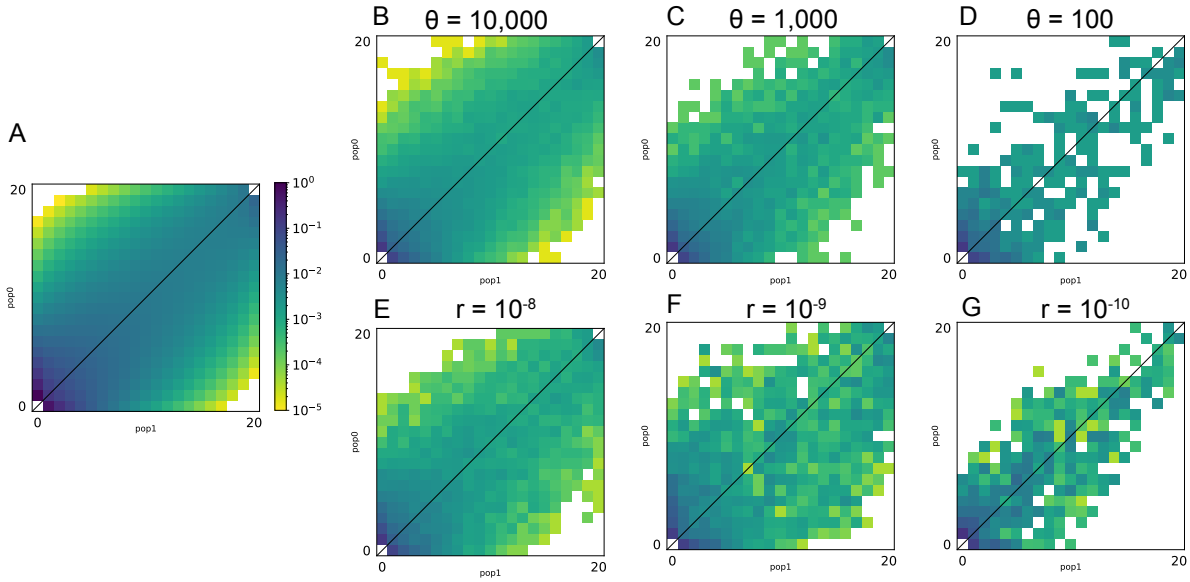

Figure S2: **Simulated AFS examples with different variance for the split-migration model**. All AFS are normalized and plotted on the same scale. (A) Expected AFS generated by dadi with $\nu_1 = 1$, $\nu_2 = 0.5$, $T = 2$, $m = 5$. (B-D) AFS with different variance by Poisson-sampling from (A). (E-G) msprime-simulated AFS with equivalent demography as in (A) under varying recombination rates. Entries below 10^{-5} are masked.

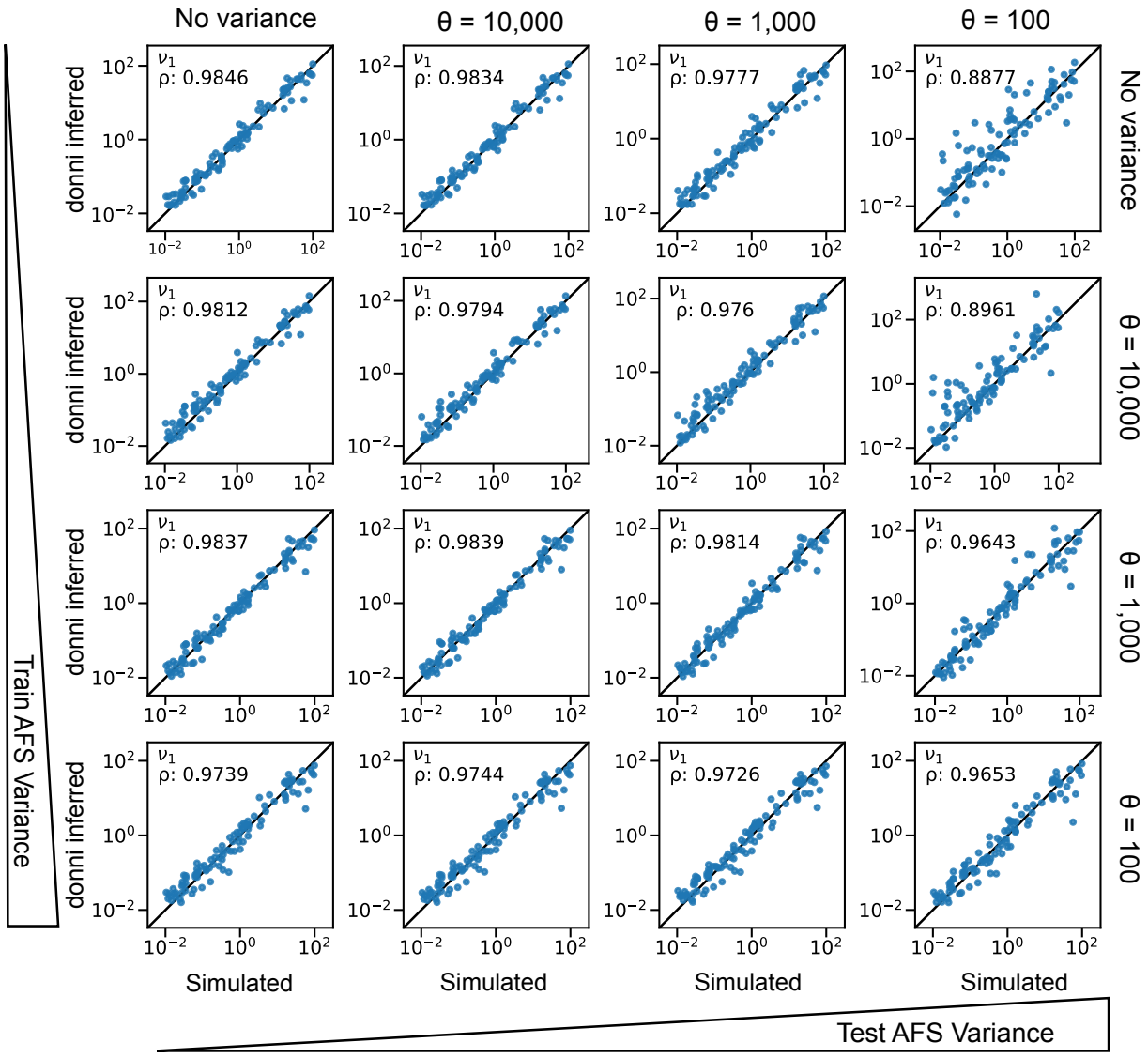

Figure S3: **The effects of AFS variance on donni training and performance for the split-migration model size-change parameter** ν_1. Each row corresponds to different levels of variance in training AFS, and each column corresponds to different levels of variance in test AFS. For example, the third panel from the left in the top row is the inference accuracy of an MLP trained on AFS with no variance tested on AFS with moderate levels of variance ($\theta = 1000$).

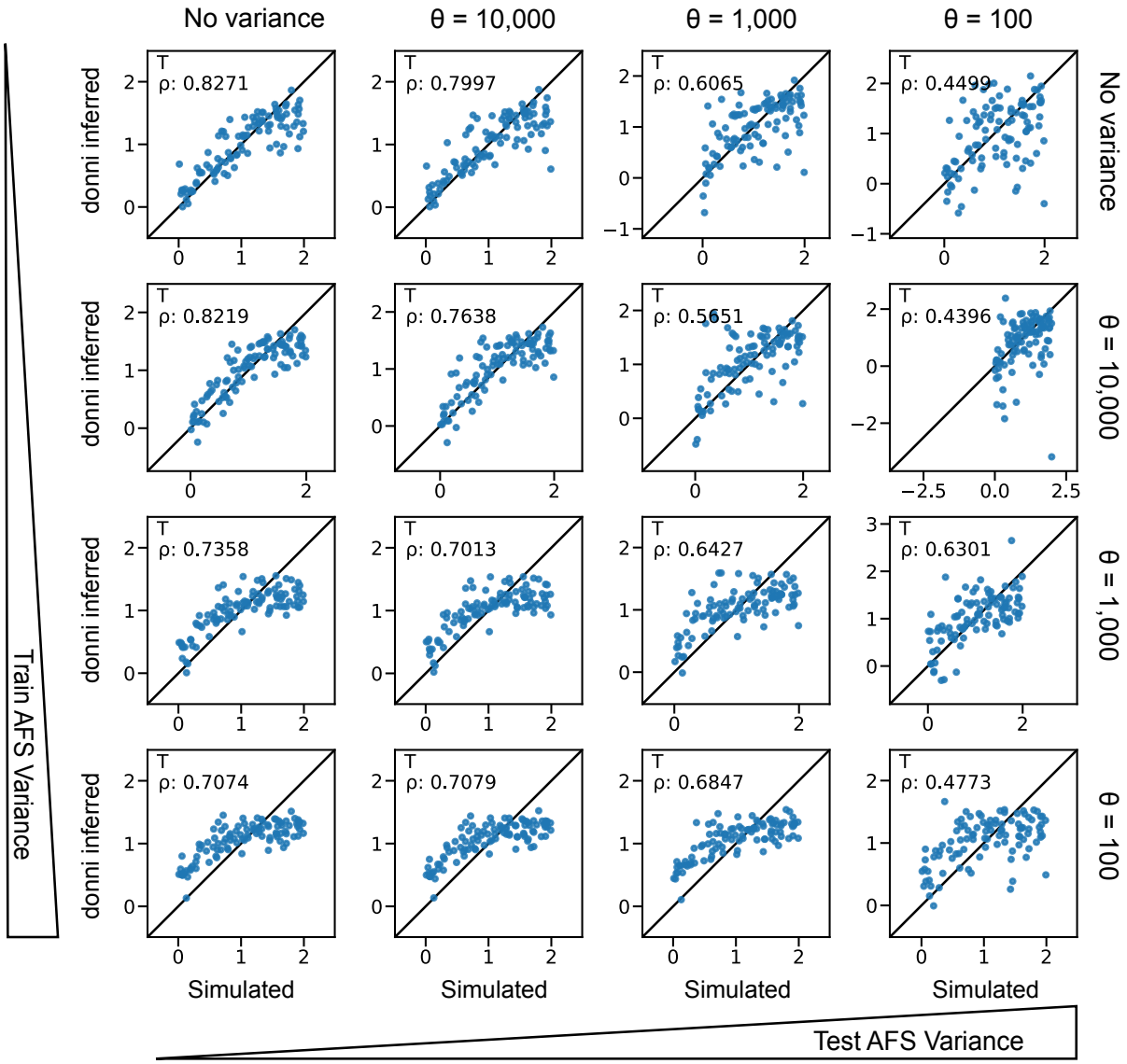

Figure S4: **The effects of AFS variance on donni training and performance for the split-migration model time parameter** T. Panels are as in Fig. S3.

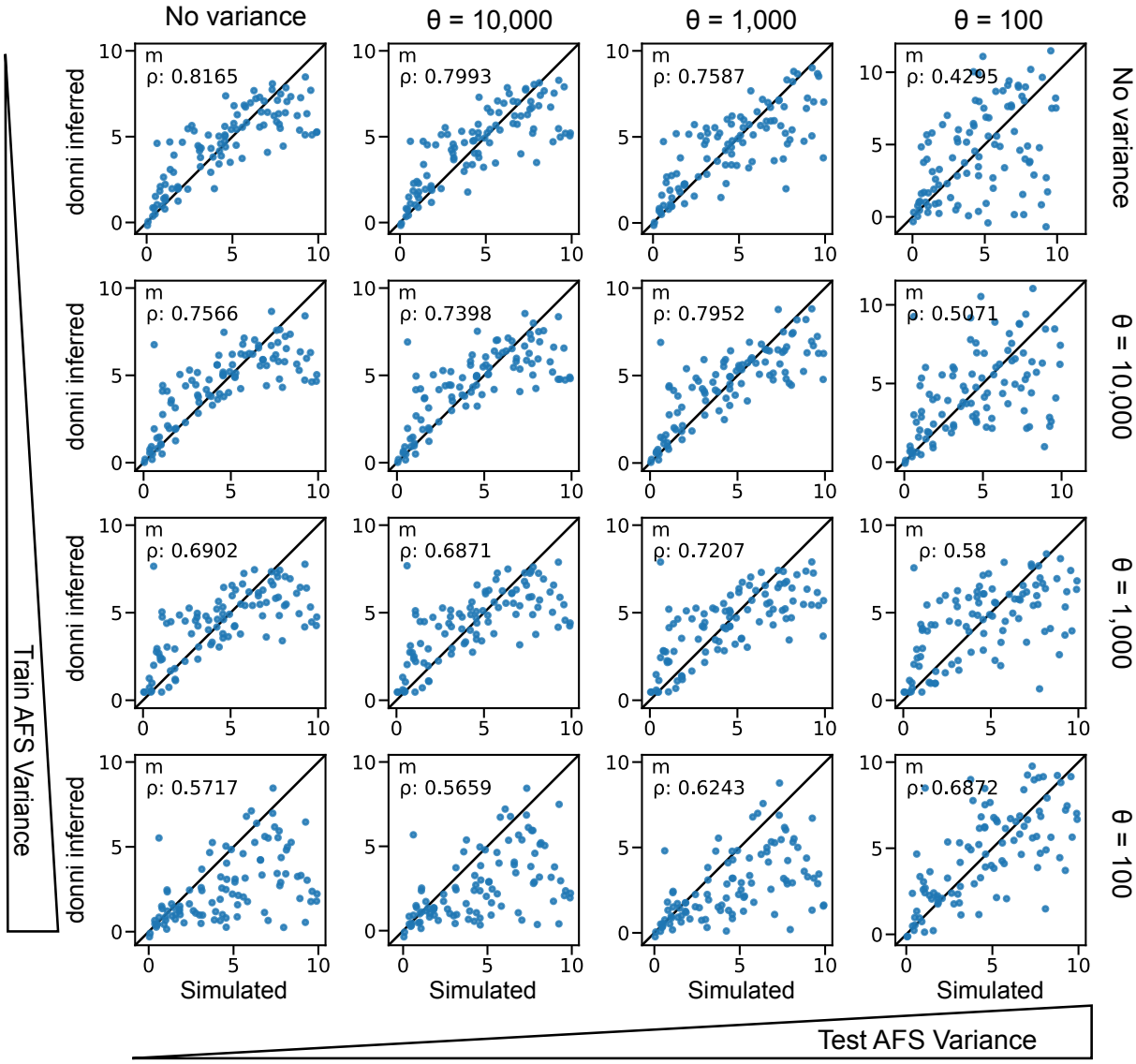

Figure S5: **The effects of AFS variance on donni training and performance for the split-migration model migration rate parameter** m. Panels are as in Fig. S3.

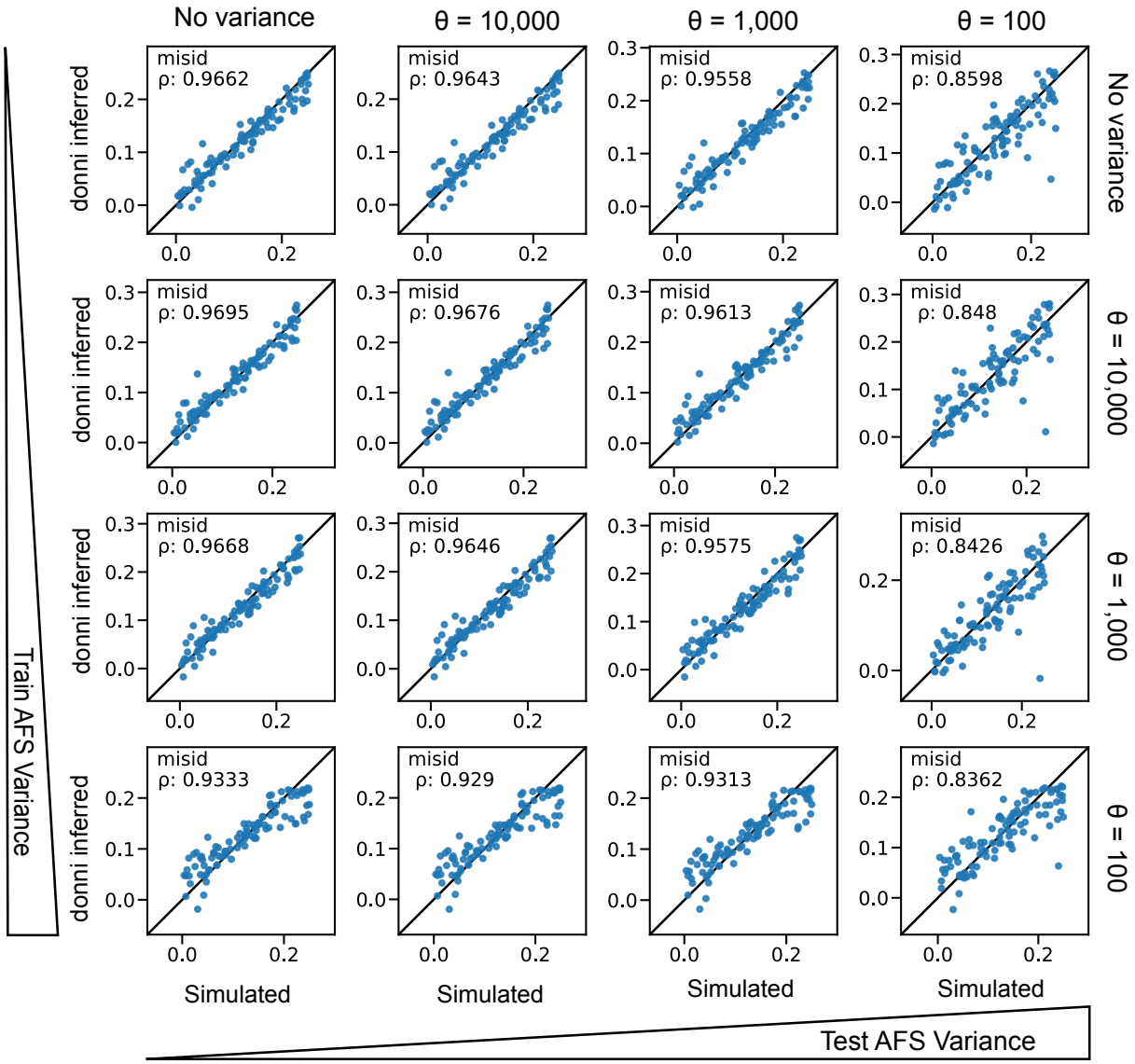

Figure S6: **The effects of AFS variance on donni training and performance for the split-migration model ancestral state misidentification parameter**. Panels are as in Fig. S3.

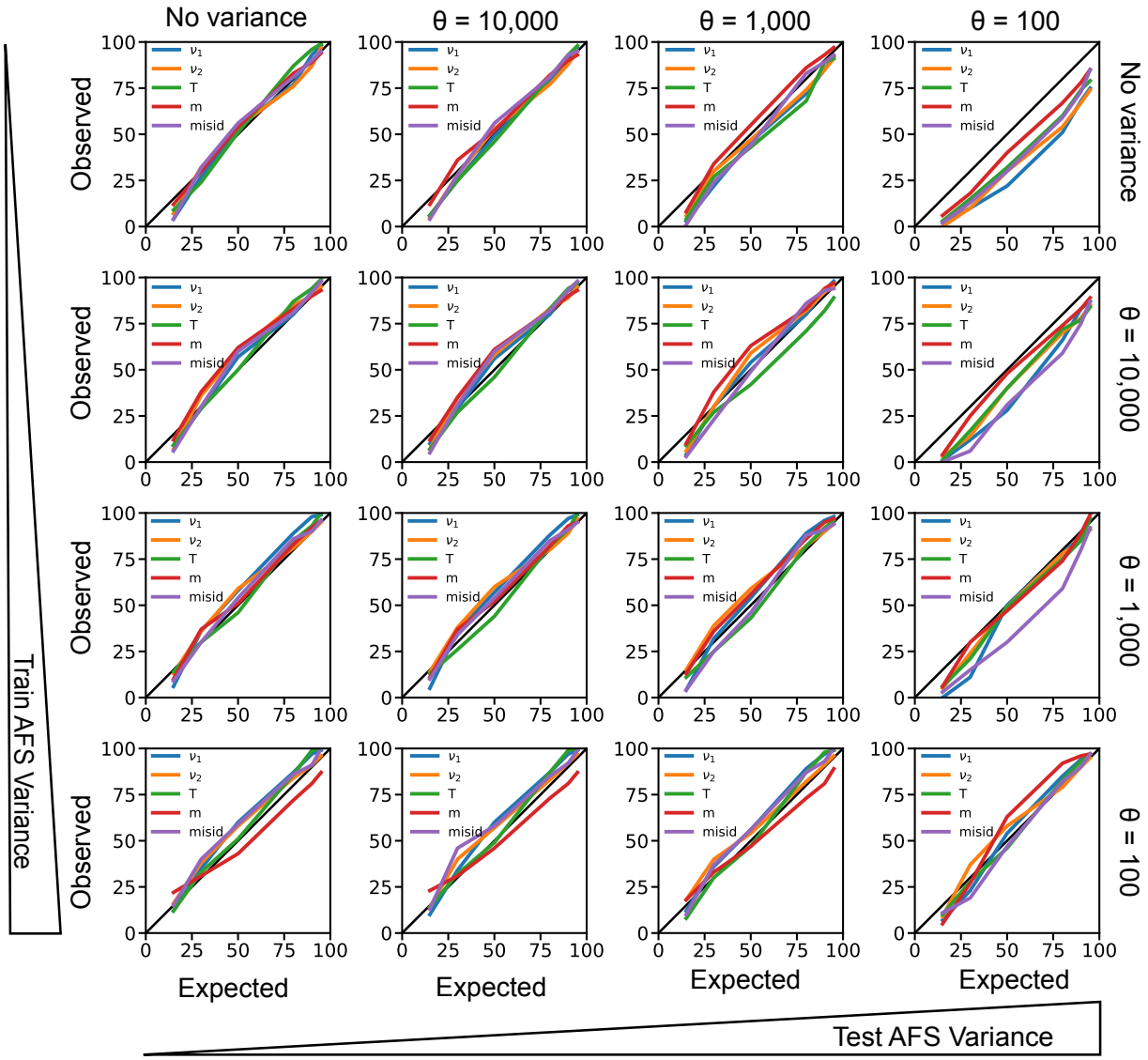

Figure S7: **The effects of AFS variance on donni's uncertainty quantification method for the split-migration model**. Panels are as in Fig. S3.

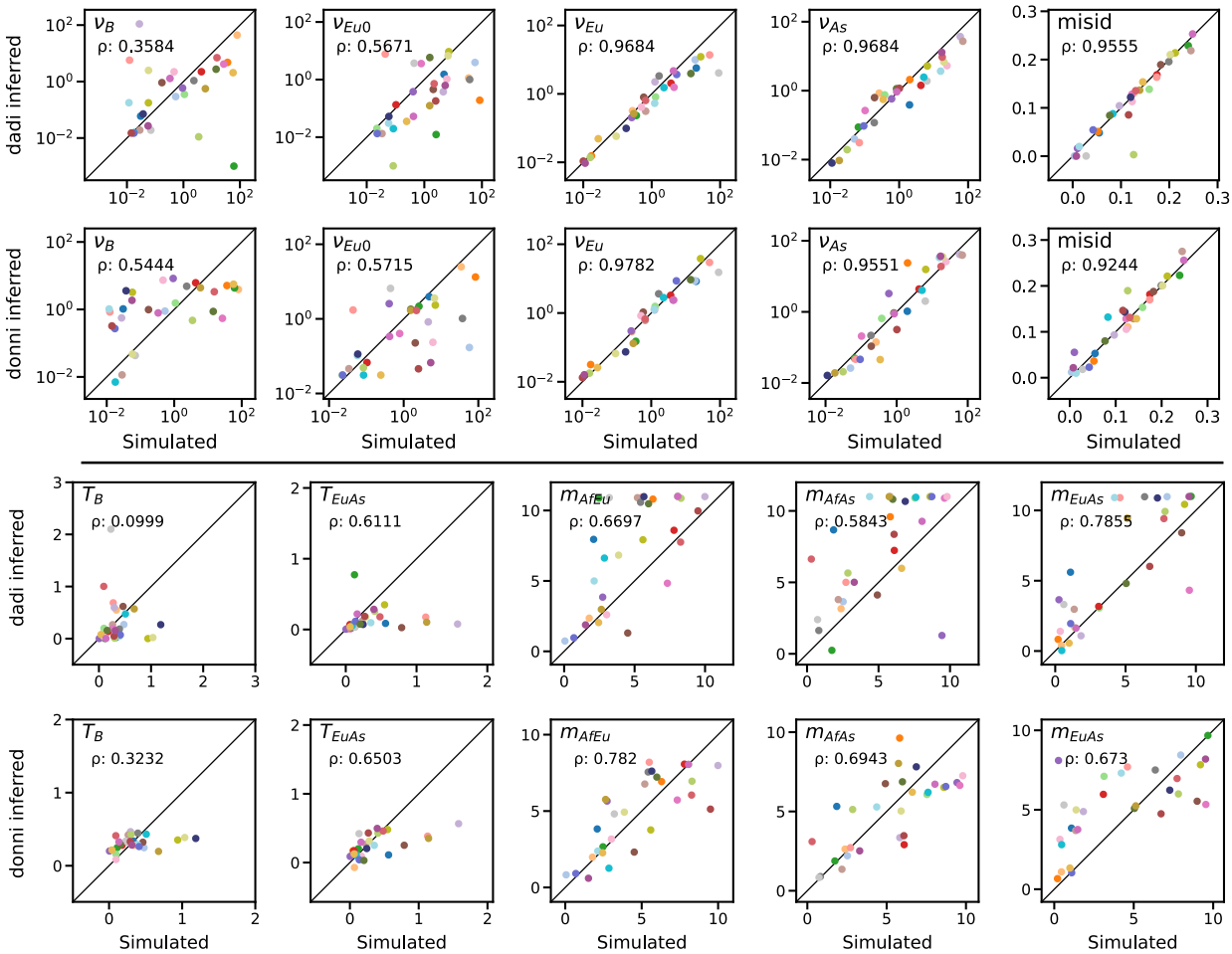

Figure S8: **Inference accuracy of dadi and donni on the rest of Out-of-Africa model parameters**.

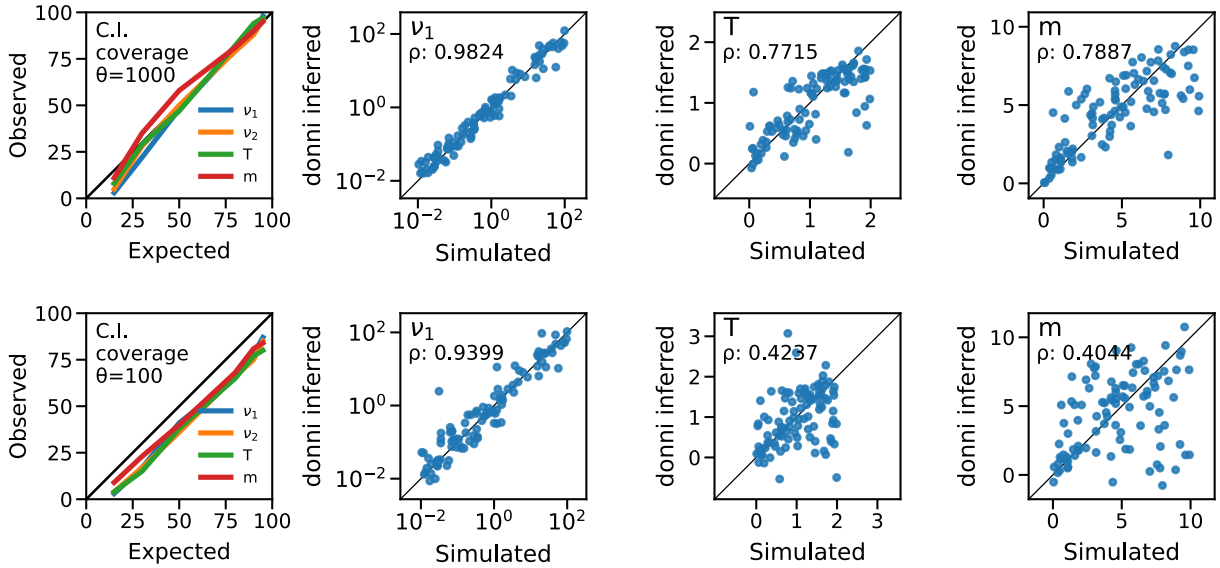

Figure S9: **Inference accuracy and confidence interval calibration by donni on down-projected test AFS for the split-migration model**. We simulated 100 test AFS with sample size 39 chromosomes per population then projected them to sample size 20 chromosomes per population. Top row is the result for test AFS projected from moderate variance ($\theta = 1000$) AFS and bottom row is for test AFS projected from high variance ($\theta = 100$) AFS.

Table S1: donni prediction accuracy on 1000 test AFS with medium variance ($\theta = 1000$) for demographic history models in this study.

Model	**Parameter**	**RMSE**	ρ
1D Two epoch	ν	8.75	0.722
	T	0.818	0.459
	misid	0.034	0.898
2D Split Migration	ν_1	8.671	0.978
($ns = 20$)	ν_2	11.055	0.977
	T	0.436	0.694
	m	2.011	0.722
	misid	0.022	0.958
2D Split Migration	ν_1	6.349	0.986
($ns = 160$)	ν_2	5.39	0.987
	T	0.436	0.637
	m	1.755	0.787
	misid	0.017	0.974
3D Out of Africa	ν_{Af}	11.914	0.985
	ν_B	22.771	0.511
	ν_{Eu0}	22.284	0.532
	ν_{Eu}	14.567	0.916
	ν_{As0}	188.784	0.499
	ν_{As}	13.886	0.932
	T_{Af}	0.3	0.428
	T_B	0.313	0.39
	T_{EuAs}	0.298	0.598
	m_{AfB}	2.87	0.117
	m_{AfEu}	1.905	0.756
	m_{AfAs}	2.026	0.718
	m_{EuAs}	2.396	0.633
	misid	0.015	0.98

Table S2: dadi demographic parameter range used for simulation in this study.

Parameter	**Symbol**	**Lower bound**	**Upper bound**
Population size change	ν	0.01	100
Time of event(*)	T	0.01	2
Migration rate	m	0	10
Ancestral state misidentification	*misid*	0	0.25

* For models with more than one T parameter, the range specified for time T applies to the sum of all T parameters (T_{sum}). For each demographic model, we drew different T_{sum} values according to the desired number of data sets. For each data set, we then drew a set of T parameters that sum to T_{sum} by sampling from the Dirichlet distribution.

Table S3: donni network architecture options for tuning based on input AFS size. Each number in the hidden layer size (HLS) options is the number of neurons in one hidden layer. Each network architecture is separated by parentheses.

Input AFS size	**Example # populations & sample size**	**HLS tuning options**
$<$ 80 entries	1 population, 10 chromosomes 1 population, 20 chromosomes 1 population, 40 chromosomes	(5,), (5,2) (10,), (10,5) (20,), (20,10)
80 $\leq$ entries $\leq$ 100	1 population, 80 chromosomes 2 populations, 10 chromosomes ea	(40,), (40,20), (40, 20,10) (50,), (50,25), (50, 25, 12)
100 $<$ entries $<$ 200	1 population, 160 chromosomes	(50,), (50,25), (50, 25, 12)
$\geq$ 200 entries	2 populations, 20 chromosomes ea ... 3 populations, 20 chromosomes ea	(50,), (50,25), (50, 25, 12), (25,), (25,12), (25,12,6)

Table S4: Hyperparmeters tuned with Hyperband for each demographic model parameter.

Hyperparameter	**scikit-learn variable**	**Value range**
Network architecture	`hidden_layer_size`	(5,) to (50, 25, 12)
Optimization algorithm	`solver`	lbfgs or adam
Initial learning rate	`learning_rate_init`	loguniform, $(10^{-5}, 0.1)$
L2 regularization term	`alpha`	loguniform, $(10^{-5}, 0.1)$